journal

J. Am. Ceram. Soc., **88** [10] 2839–2847 (2005)
DOI: 10.1111/j.1551-2916.2005.00641.x
© 2005 The American Ceramic Society

Processing Effects for Integrated PZT: Residual Stress, Thickness, and Dielectric Properties

Ryan J. Ong*,† and David A. Payne**

Department of Materials Science and Engineering and Frederick Seitz Materials Research Laboratory, University of Illinois at Urbana-Champaign, Urbana, Illinois 61801

Nancy R. Sottos

Department of Theoretical and Applied Mechanics, University of Illinois at Urbana-Champaign, Urbana, Illinois 61801

Processing effects on the dielectric properties of sol–gel-derived $PbZrO_3$–$PbTiO_3$ (PZT) films integrated onto $Pt/Ti/SiO_2//Si$ substrates are reported. Sol–gel synthesis and deposition conditions were designed to produce films of varying thickness (95–500 nm) with consistent chemical composition ($Pb(Zr_{0.53}Ti_{0.47})O_3$), phase content (perovskite), grain size (∼110 nm), crystallographic orientation (nominally (111) fiber textured), and measured residual stress. The Stoney method, using laser reflectance to determine wafer curvature, derived biaxial tensile stress values of 150 and 180 MPa for PZT films after a baseline correction for electrode interactions during thermal processing was employed. The PZT films were of high dielectric quality, with low losses and negligible dispersion. Calculated values of dielectric constant ($\bar{K}'$) were found to decrease from 960 to 600 with decreasing film thickness. A series-capacitor model successfully recovered a room-temperature K'_1 for the PZT (1,170) in good agreement with bulk reports but was unable to reproduce the expected dielectric anomaly near 380°C. This discrepancy and the resulting diffuse phase transformation were attributed to the biaxial tensile stress present in the PZT films.

I. Introduction

The properties of films are often different than bulk materials of the same composition. Potential reasons for this discrepancy are considered in this paper, including processing effects on properties. Compositions in the $PbZrO_3$–$PbTiO_3$ (PZT) system are used in capacitors, piezoelectric transducers, and pyroelectric detectors.[1] Direct integration of PZT films on Si leads to additional functionalities for the integrated circuit, including on-chip power capacitors, vibration sensors, and infra-red imaging.[2,3]

Measurements have demonstrated differences in the properties of integrated PZT films when compared with bulk values, and explanations have been proposed, including changes in chemical composition, phase content, grain size, crystallographic orientation, thickness, and stress.[4–9] Of the aforementioned variables, the residual stress state in a polycrystalline film is the most difficult to assess, but necessary to consider. For example, applied mechanical stresses of 30 MPa have been demonstrated to have a measurable effect on the dielectric, ferroelectric, and piezoelectric response of PZT films.[10–12] Previous research has indicated that between 100 and 200 MPa of biaxial tensile stress may be present in PZT films deposited onto $Pt/Ti/SiO_2//Si$ substrates and are expected to alter the film's properties.[9–11,13] Unfortunately, to date, the separation of processing-induced residual stress effects from the other aforementioned variables has been difficult to accomplish.

We report here data for sol–gel-derived $Pb(Zr_{0.53}Ti_{0.47})O_3$ films integrated onto $Pt/Ti/SiO_2//Si$ substrates. A processing methodology was designed to control variations in chemical composition, phase content, grain size, and crystallographic orientation in order to separate thickness and residual stress effects. X-ray diffraction (XRD) and scanning electron microscopy (SEM) were used to determine the success of film processing. Residual stress was measured by a wafer curvature method. A series-capacitor model accounted for the observed decrease in room-temperature dielectric constant (K) as film thickness (t_f) decreased. However, a discrepancy between film and bulk behavior remained in the temperature dependence of K, attributable to processing-induced residual stress (σ), and was separated in polycrystalline PZT films for the first time in this work.

II. Background Information

Thin films can be deposited by physical or chemical methods, in vacuum or ambient atmospheres. Widely used techniques include sputter deposition,[14] pulsed laser deposition,[15] metalloorganic chemical vapor deposition,[16] hydrothermal growth,[17] and chemical-solution deposition,[18] of which sol–gel processing can be considered a subset.[19] For the current investigation, a polymeric sol–gel route was used for attributes of low cost, liquid-phase mixing at the molecular level, and control of purity, stoichiometry, and homogeneity in a contained system. In addition, the sol–gel route facilitates the processing of oxide materials in oxidizing atmospheres and the ability to coat large diameter substrates by spin-casting methods.[20]

Previous work has shown that sol–gel-derived PZT films react with silicon when in direct contact ($PZT/SiO_2//Si$), resulting in the formation of lead silicate and PZT–pyrochlore-type phases, with cracking of films greater than 280 nm thick.[21,22] Residual tensile stresses of 110 MPa were determined and observed cracking was attributed to the formation of interfacial reaction products. $Pt/SiO_2//Si$ substrates were successful in arresting PZT and SiO_2 reactions, but adhesion problems between the Pt and SiO_2 were of concern.[23] For example, as-deposited Pt was observed to release from the surface of $SiO_2//Si$ after several weeks at room temperature. A 120 nm thick PZT (perovskite plus pyrochlore) film deposited onto $Pt/SiO_2//Si$ had a measured σ of 400 MPa.[23] Phase purity was not achieved, attributed to the loss of PbO

S. J. Glass—contributing editor

Manuscript No. 20465. Received September 26, 2004; approved May 4, 2005.
Based in part on the thesis submitted by R. J. Ong for the Ph.D. degree in Materials Science and Engineering, University of Illinois, Urbana, IL, 2005.
Presented at the 106th Annual Meeting of The American Ceramic Society, Indianapolis, IN, April 20, 2004, in the symposium in honor of Ed Fuller.
This work was supported by the National Science Foundation through grant CMS 00-8206, the U.S. Department of Energy, Division of Materials Sciences under Award No. DEFG02-91ER45439, through the Frederick Seitz Materials Research Laboratory at the University of Illinois at Urbana-Champaign.
*Member, American Ceramic Society.
**Fellow, American Ceramic Society.
†Author to whom correspondence should be addressed. e-mail: ryan.j.ong@intel.com

during thermal processing. For improved adhesion, a Ti bonding layer is commonly used in device integration. This results in the $Pt/Ti/SiO_2//Si$ structure, often referred to as "platinized silicon," used in this work.

The weak-field dielectric properties of polycrystalline PZT films are often reported to be inferior to those measured on bulk ceramics, regardless of the method of deposition. For example, the K of PZT is known to decrease as film thickness drops below 1 μm.[8] Variations in chemical composition, phase content, grain size, preferred orientation, and residual stress have all been considered as possible reasons for these discrepancies. A composition ($Pb(Zr_{0.53}Ti_{0.47})O_3$) close to the morphotropic phase boundary (MPB) was chosen in the present work because of the large K ($>10^3$) measured for bulk specimens.[24] Dilution of K by phase mixing can occur in high-K ceramics and films.[8,25,26] Effects of crystallographic orientation on properties have been reported for anisotropic PZT.[7] The development of stress on cooling from the high-temperature cubic phase has shown domain-orientation effects in tetragonal PZT films, a-axis extension normal to the film for tensile stress, and c-axis extension for compressive stresses.[27] Other reports have shown that application of external stresses can change the properties of polarizable and deformable ceramic films.[10–12,28,29] Garino and Harrington[10] reported a reversible 2% change in K when the residual tensile stress was reduced by 30 MPa. Similar results were reported by Kanno *et al.*[29] for c-axis PZT films, when a one-dimensional stress resulted in a 5% change in K over a 150 MPa range. These reports indicate that any change in K with stress may be minor at room temperature. An even greater effect was observed by Lian and Sottos[12] for the piezoelectric response of PZT films, where the application of 44 MPa of tensile stress (in addition to the residual stress) reduced the field-induced strain by 26%. The opposite trend was observed for applied compressive stress, i.e. field-induced strain increased. Furthermore, recent work has extended the concepts of Buessem *et al.*[30,31] on the interplay between mechanical stresses and dielectric properties from bulk ceramics to epitaxial films. These articles suggested that both the transformation temperature and the temperature variation of K can be affected by stress.[29,32–35]

The quantification of stress development during sol–gel processing is less known when constrained shrinkage occurs during drying and firing.[20,22,36] However, on cooling, thermal stresses can be estimated from

$$\sigma_f(T_0) - \sigma_f(T) = E(T_0 - T)(\alpha_f - \alpha_s)(1 - 3j + 6j^2) \quad (1)$$

where σ_f is the stress that develops in a constrained film from temperature T_0 to T. E is Young's modulus for the film, while α_f and α_s are the thermal expansion coefficients for the film and substrate, respectively.[37] The ratio of film to substrate thickness is j. For example, a 500 nm $Pb(Zr_{0.53}Ti_{0.47})O_3$ film ($E = 70$ GPa, $\alpha = 4.8 \times 10^{-6}$°C^{-1})[24,38] adhered to a 375 μm Si substrate ($\alpha = 3.5 \times 10^{-6}$°C^{-1}),[38] is estimated to develop a tensile stress of 60 MPa from thermal expansion mismatch on cooling from 650°C to room temperature. This calculation assumes a stress-free film at 650°C, which is most certainly not the case because of prior shrinkage on heating. A similar calculation by Lian, but for a stress-free condition at 750°C, and using a recursive calculation involving the temperature-dependent expansion properties of both the $Pb(Zr_{0.52}Ti_{0.48})O_3$ (bulk) and Si, resulted in a 75 MPa biaxial tensile stress attributable to thermal expansion mismatch alone.[39] Lead titanate has a negative thermal expansion coefficient ($\alpha = -5.3 \times 10^{-6}$°C^{-1}) below 500°C while lead zirconate is positive ($\alpha = 12 \times 10^{-6}$°C^{-1}), and the temperature coefficients for PZT can be designed depending on composition.[24]

Experimental data indicate that tensile stresses between 100 and 200 MPa are present at room temperature for sol–gel-derived PZT films on platinized silicon.[9,10,13,40] These data, combined with the calculations presented above, indicate not only that a significant proportion of the final residual stress can be attributed to the thermal component, but also that an additional stress component must be present at high temperatures stemming from constrained shrinkage. The presence of these residual stresses, regardless of origin, is expected to affect the properties of PZT.

Determination of film thickness, phase assemblage, crystallographic orientation, and residual stress are all experimentally possible. However, specimens with a reduced set of free variables are preferred for a better understanding of processing effects on properties. The purpose of this investigation was to prepare PZT films with thicknesses ranging from 95 to 500 nm with consistent chemical composition and phase content, and to determine the grain size, crystallographic orientation, and residual stresses that resulted after thermal processing. Data are then related to the measured weak-field properties for polycrystalline PZT films.

III. Experimental Procedure

PZT films were deposited by a polymeric sol–gel method adapted from the work of Budd *et al.*[19] and Lakeman *et al.*[5] and Pb-acetate trihydrate, Zr-*n*-propoxide, Ti-isopropoxide, and 2-methoxyethanol were used as precursors. Reaction of these chemicals in a Schlenk apparatus under an inert atmosphere (dry N_2) allowed for homogenous mixing and strict control of solution stoichiometry and purity. Lead acetate trihydrate ($Pb(CH_3COO)_2 \cdot 3H_2O$) with 5 mol% PbO excess was vacuum dehydrated for 12 h at 80°C, before refluxing with 2-methoxyethanol at >100°C for 1 h. The solution was thermally distilled twice at 140°C, with redilution in 2-methoxyethanol each time, followed by two vacuum distillations at 65°C and ~ 10 Torr. Separately, Zr-*n*-propoxide and Ti-isopropoxide were refluxed with 2-methoxyethanol at >100°C for 1 h. Two thermal distillations were carried out (with redilution in 2-methoxyethanol) prior to transfer of the Zr/Ti solution to the Pb-containing solution. The combined solution was then refluxed for an additional hour prior to two thermal distillations and two vacuum distillations. The result was a light yellow viscous $Pb(Zr_{0.53}Ti_{0.47})O_3$ stock solution, and the stoichiometry was verified by ICP. This solution was cooled to room temperature, diluted with 2-methoxyethanol, and partially hydrolyzed. A molarity of 0.25 and water to alkoxide ratio (R_w) of 0.5 was chosen and held constant throughout the investigation. The partially hydrolyzed sol was allowed to age for more than 2 days before spin casting. Solutions prepared in this manner were stable for >6 months. A 0.25M $R_w = 0.5$ PbO covercoat solution was also prepared for use in controlling Pb-loss during heat treatment.[41]

Single-crystal Si (00l) substrates (single-side polished, 3″ diameter, 375 μm thick) with a thermally grown 5000 Å SiO_2 layer were purchased from Silicon Quest International Inc., Santa Clara, CA. The radius of curvature was determined on a laser-reflectance system (FLX-2908 KLA-Tencor Corporation, San Jose, CA). DC magnetron sputtering (AJA International Inc., North Scituate, MA) was used to deposit 300 Å of Ti and 1700 Å of Pt to form a well-adhered electrode layer. After metallization, the radius of curvature of the electroded silicon was remeasured, and this value was used initially in stress calculations, prior to a correction that is emphasized below.

Stoney,[42] in 1909, considered the effect of electroplating Ni on thicker steel rules, and estimated residual stress from a change in radius of curvature. Residual stress derived by this approach is given by

$$\sigma = \left(\frac{E}{1-\upsilon}\right)_s \frac{t_s^2}{6t_f}\left(\frac{1}{R} - \frac{1}{R_0}\right) \quad (2)$$

where $(E/1-\upsilon)_s$ is the known biaxial modulus for the steel substrate, t_s and t_f are the thicknesses of the substrate and film, respectively, and R_0 and R are the radii of curvature of the substrate before and after film deposition. The estimate of σ is valid if $j < 10^{-2}$ and the film is well adhered to the substrate, with no stress relief by buckling or cracking.[43] This method is

particularly attractive for films of unknown, or processing-dependent properties, adhered to a well-characterized substrate (such as single-crystal silicon). Thus, the sol–gel-derived PZT films, which were two orders of magnitude thinner than the substrate and were strongly bonded to the metallization layer, with elastic properties dependent on thermal processing conditions, were ideal candidates for analysis by the Stoney method.[9,10,13,22,36] Accurate radii-of-curvature measurements and assignment yield residual stress values for films of known thickness, without knowledge of phase purity, chemical composition, grain size, or crystallographic orientation.

PZT films were deposited by spin casting (Headway Research Inc., Garland, TX) onto platinized silicon substrates from partially hydrolyzed sols dispensed through a filtered syringe. Solution was metered onto a rotating substrate at 300 rpm before accelerating to 3000 rpm for 60 s, producing a layer of uniform coverage. The as-spun layer was on the order of 90 nm in thickness. After spin coating, thermal treatments on a hotplate in air at 120°C for 1 min, and at 300°C for 1 min, were used to dry and pyrolyze the metalloorganic material, resulting in a metal oxide film of less than half the original thickness. The procedure was then repeated to build up thicker layers. Up to four layers at a time could be deposited, dried, and pyrolyzed in this manner, prior to higher-temperature crystallization (650°C). Increasing the number of pyrolyzed layers beyond this point led to cracking on crystallization. Previous results indicated that 5 mol% excess PbO in solution was insufficient to compensate for Pb loss during higher-temperature processing.[23] A Pb deficiency is often linked to the formation of a pyrochlore or defect-fluorite phase instead of the desired perovskite phase.[41] Therefore, prior to the crystallization treatment, a PbO covercoat was spun over the PZT film to assist in complete perovskite phase formation during heat treatment.[41] The PZT layer with covercoat was heat treated at 650°C for 30 min. After crystallization, the PZT films were rinsed in acetic acid and cleaned with 2-methoxyethanol to remove any residual lead oxide particles that might have persisted on the surface. This methodology produced uniform, crack-free films, in a consistent manner. Furthermore, the deposition, heat treatment, and rinse cycles were standardized and repeated to build up thicker films. For example, a final film thickness of 95 nm was achieved by drying and pyrolyzing two layers, followed by a PbO covercoat, a crystallization heat treatment, and acetic acid rinse. To achieve a 190 nm PZT film, four layers were deposited, dried, and pyrolyzed prior to crystallization and acetic acid treatment. These films only experienced one high-temperature crystallization treatment. However, the 350 and 500 nm films consisting of eight and 12 total layers, respectively, were crystallized after each four-layer set. Thus, these films were not crystallized in one heat treatment, but rather in a step-wise fashion, building from previously deposited material.

After crystallization and cooling, the radius of curvature was re-determined and compared with the baseline curvature for the metallized substrate before PZT deposition and firing. The sole use of the baseline curvature for the "as-deposited" Pt/Ti/SiO_2//Si substrate complicates analysis. Spierings *et al.*[9] and Zhang *et al.*[13] reported on the need for correction of the baseline curvature (R_0) when determining residual stresses in PZT films deposited on Pt/Ti/SiO_2//Si substrates. In each case the PZT film was removed after crystallization to reveal the curvature of the underlying substrate. The present work followed their approach, and at least two identical PZT/Pt/Ti/SiO_2//Si specimens were prepared for each thickness so that one could be used for further analysis, and the other could have the PZT film etched away to determine the radius of curvature of the Pt/Ti/SiO_2//Si after thermal processing. Removal of the PZT film was achieved in aqueous solution of hydrochloric acid with ammonium bifluoride. The etching process resulted in the recovery of a clean Pt/Ti/SiO_2//Si substrate with a mirror-like finish suitable for characterization by laser reflectance. The methodology allowed for the calculation of the true residual stress in PZT films, which could then be related to measured dielectric properties to determine what effects, if any, were present.

XRD analysis was carried out on an X'Pert MRD (PANalytical, Natick, MA) with Cu$K\alpha$ radiation and a Ni filter. Standard 2θ–ω scans were acquired for each film after aligning the specimen with the sharp Si (004) peak in order to detect crystalline phases. Field emission SEM revealed microstructural features on a Hitachi S4700 (Pleasanton, CA) at an accelerating voltage of 10 kV for plan view and 15 kV for cross-sectional specimens. A sputtered Au/Pd layer was used to reduce charging effects on all specimens. Plan-view photomicrographs were used to calculate average grain size using the ASTM E112-96 line-intercept method, with over 100 grains counted per specimen.[44] Cross-sectional analysis enabled an accurate determination of film thickness, with verification of grain size and phase content.

Prior to electrical measurements, Pt top electrodes were DC sputtered through a shadow mask onto the PZT surface to form a parallel-plate capacitor configuration. A Precision LCR meter (Hewlett-Packard 4284A, Palo Alto, CA), with custom written automation program, was used to gather capacitance data at room temperature as a function of frequency from 100 Hz to 100 kHz (AC = 50 mV, DC = 0 V), and separately as a function of temperature at 100 kHz from 50° to 450°C at heating and cooling rates of 1°C/min (data taken in 0.25°C increments).

IV. Results and Discussion

Processing steps were designed to integrate $Pb(Zr_{0.53}Ti_{0.47})O_3$ films onto Pt/Ti/SiO_2//Si in a reproducible and consistent manner. A common stock solution with a fixed composition was used with identical steps throughout the processing cycle. The methodology facilitated the deposition of PZT films of varying thicknesses while keeping chemical composition constant. Furthermore, grain size, phase content, crystallographic orientation, and residual stress were determined for all specimens. We start by considering residual stress.

Stress present in sol–gel-derived films stems from constrained shrinkage on a rigid substrate as a wet film gels, dries, is pyrolyzed, densified, crystallized, and finally cooled (with thermal expansion mismatch between the film and substrate) to room temperature.[9,10,13,20,22,36] PZT/Pt/Ti/SiO_2//Si specimens were prepared with $t_f = 95$, 190, 350, and 500 nm. Thus, with known film and substrate thicknesses, and known elastic properties for the substrate, the calculation of residual stress from radius of curvature measurements and the Stoney equation appears straightforward.[42] However, accuracy depends on the precise determination and assignment of R_0 in Eq. (2).[9,13]

The reference radius of curvature (R_0) in the Stoney equation is assigned to the Pt/Ti/SiO_2//Si substrate. Table I lists measured R values used in calculations of residual stress and the resulting calculated stress values. Variability exists in the initial values of R_0 for the as-sputtered Pt/Ti/SiO_2//Si because of differences in the as-received SiO_2//Si substrates. However, this variability was measured and accounted for during residual stress calculations. A biaxial elastic modulus of 1.805×10^{11} Pa was used for Si substrates.[45] Figure 1 depicts the calculated residual stress in PZT films if the radius of the "as-sputtered" Pt/Ti/SiO_2//Si substrate was used as the reference, compared with later values determined after the PZT had been etched away, i.e., the radius of curvature had been re-determined for the now heat-treated Pt/Ti/SiO_2//Si substrate. Unreasonably high values of residual stress were calculated for the PZT film when the as-deposited Pt/Ti was used as a reference (upper trace). The calculated values, reaching into the GPa range, would correspond to tensile strains $>3\%$, an order of magnitude greater than the strain to failure. This erroneous calculation is attributed to reactions in the Pt/Ti layer.

Previous work indicated that reactions take place between Pt and Ti on heat treatment.[10,46] A chemical reaction or physical rearrangement could change the radius of curvature and the subsequent estimate of σ. Furthermore, the ratio of PZT thickness to Pt/Ti thickness also affects calculated stress values. For example, the bending moment induced by a 200 nm Pt/Ti layer

Table I. Radii of Curvature used in Calculations of Residual Stress

PZT film thickness (nm)	R_0 for as-sputtered Pt/Ti/SiO_2//Si (m)	R_0 for recovered Pt/Ti/SiO_2//Si (m)	R for PZT deposited on Pt/Ti/SiO_2//Si (m)	Calculated stress in PZT, using R_0 for the as-sputtered substrate (MPa)	Calculated stress in PZT, using the corrected R_0 for the recovered substrate (MPa)
95	−31.6	41.0	35.3	2670	180
190	−15.3	−469.7	168.0	1590	180
350	−149.0	19.8	15.8	850	150
500	−21.3	81.3	32.9	650	150

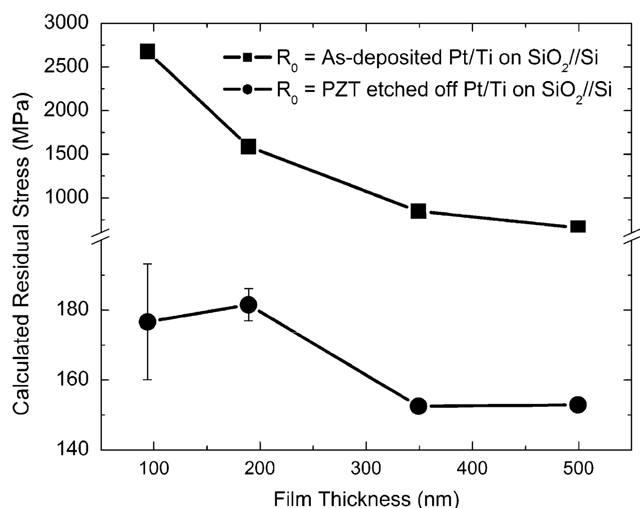

Fig. 1. Calculated stress for PZT films of different thicknesses with (a) R_0 = as-deposited Pt/Ti on SiO_2//Si and (b) R_0 = PZT etched off heat-treated Pt/Ti on SiO_2//Si.

is proportionately larger for a 95 nm thick PZT film than for a 500 nm thick PZT film. Therefore, if the bending moment from the Pt/Ti layer was not correctly accounted for, residual stress values would be overestimated. Calculated stress levels would eventually decrease to an asymptotic value as PZT film thickness increased and the contribution from the Pt/Ti layer was diluted.

As mentioned, at least two identical 3″ wafers were processed for each desired PZT film thickness. One wafer was used for later analysis (XRD, SEM, electrical measurements, etc.), while the other had the PZT film etched away from the wafer to determine the appropriate R_0. The lower trace in Fig. 1 illustrates the calculated stress (150–180 MPa) in the PZT film using corrected reference curvatures. (Recall the previous estimate of thermal stress was between 60 and 75 MPa, tension.) Residual stress values calculated in this work are in qualitative agreement with previous results (100–200 MPa, tension) for solution-derived PZT films.[9,10,13] By combining the residual stress measurements with the estimates of stress because of thermal expansion mismatch, it is possible to say that a tensile stress is present at all times during cooling from 650°C (the highest processing temperature). Before any meaningful interpretation can be put forth, the phase content, grain size, and crystallographic orientation of the PZT films must be reported.

Figures 2 and 3 illustrate the microstructures of PZT films. Dense, homogenous microstructures were observed throughout this investigation. Film thicknesses were determined from cross-sectional analysis (Fig. 2). Results indicated the thinnest film (t_f = 95 nm) was one grain thick. As thickness increased, a strictly columnar microstructure was not observed. Instead, a “brick-wall” type of microstructure evolved. For example, four distinct layers are present in the 500 nm film. Each layer is comprised of columnar grains, with no registry evident between the layers. The average diameter of grains in this cross-section was ~110 nm with no observable difference between layers. Relatively few intercepts were available in the cross-sectional analysis and the precise determination of grain boundaries was difficult.

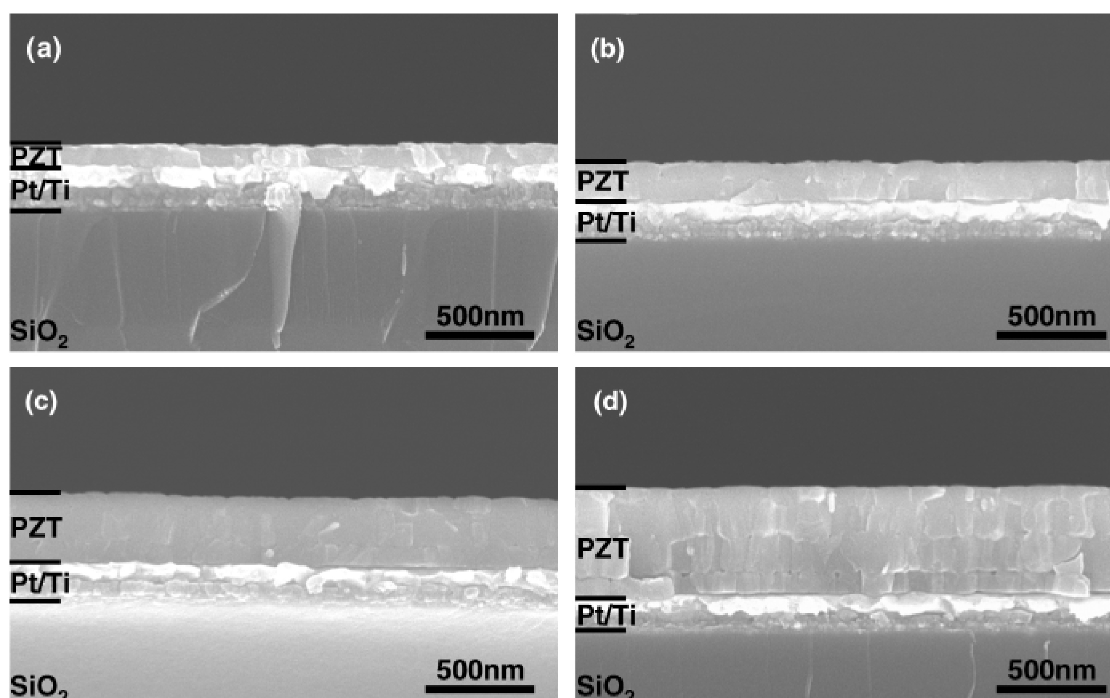

Fig. 2. Scanning electron photomicrographs (cross-sectional views) of (a) 95 nm, (b) 190 nm, (c) 350 nm, and (d) 500 nm PZT films.

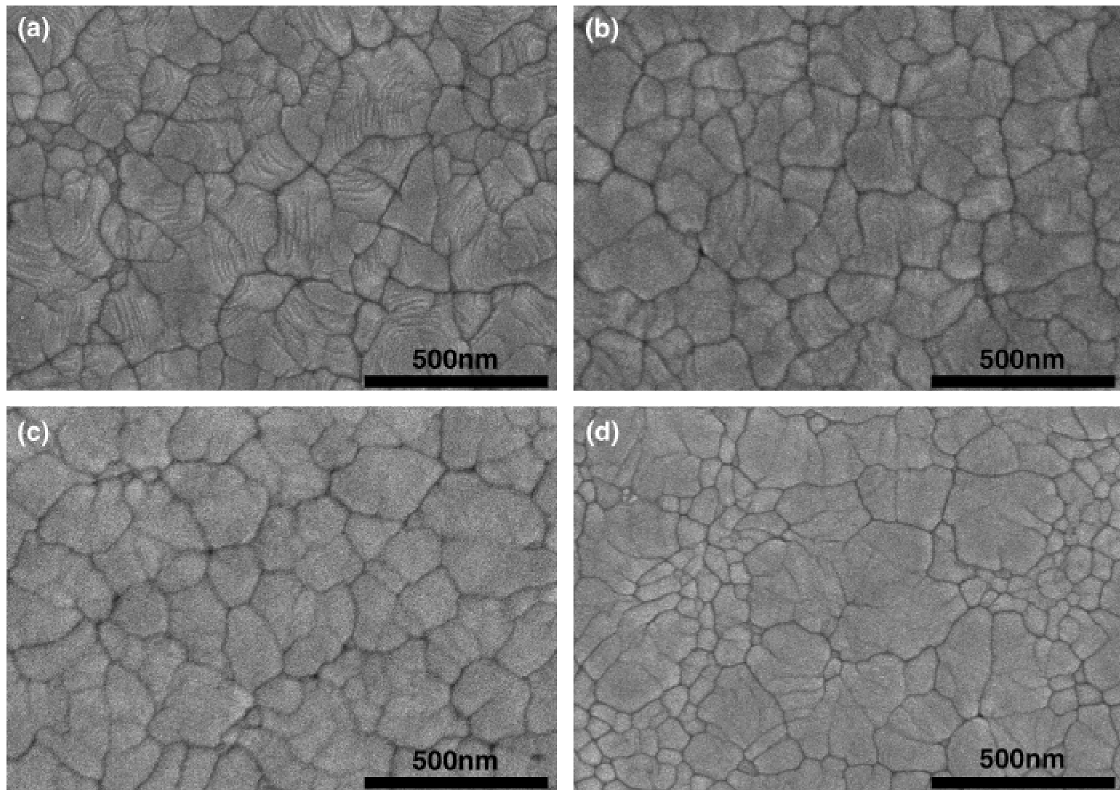

Fig. 3. Scanning electron photomicrographs (plan views) of (a) 95 nm, (b) 190 nm, (c) 350 nm, and (d) 500 nm PZT films.

The error for cross-sectional analysis was estimated at ± 20 nm. Estimates of average grain diameter determined for the volume of the film are in good agreement with those calculated from surface micrographs, where a larger number of grains were counted (Fig. 3). Determinations of surface grain size were 115, 120, 100, and 115 nm (with an uncertainty of ± 10 nm) as t_f increased from 95 to 190, 350, and 500 nm. Importantly, a bimodal distribution observed in the 500 nm PZT surface micrograph (Fig. 3(d)) was not apparent in the volume of the film (Fig. 2(d)). Thus, it is possible that the bimodal observation was largely a surface artifact, with the bulk of the film containing grains with an average diameter of ~ 110 nm. We conclude that there was no significant difference in grain size between the different films. The average surface grain size of the Pt/Ti metallization layer was found to be 35 nm after etching away the heat-treated PZT. There was also no significant difference in grain size for the electrode material between the different specimens.

Figure 4 gives XRD data (2θ–ω) obtained from the films of different thicknesses. Note that a semi-log scale representation is used to accentuate the lower intensity peaks from the film that would normally be masked by the higher intensity substrate (Pt and Si) peaks. All reflections were assigned to either the substrate or perovskite $Pb(Zr_{0.53}Ti_{0.47})O_3$. Crystalline secondary phases (such as a defect fluorite or pyrochlore) were not detected by XRD, or observed by SEM. Thus, given the long collection times used and the semi-log scale display, the data indicate single-phase perovskite with a pseudocubic lattice constant of 4.07 Å for all specimens. The calculated pseudocubic lattice constant and the overall XRD pattern compares favorably with both tetragonal and rhombohedral $Pb(Zr_{0.53}Ti_{0.47})O_3$ (JCPDS 01-070-4264 with $a = 4.04$ Å and $c = 4.13$ Å giving $\sqrt[3]{a^2c} = 4.07$ Å, and JCPDS 01-070-4265 with $a = 4.08$ Å, $\alpha = 89.83°$) as well as the pseudocubic $a = 4.08$ Å for gel-derived $Pb(Zr_{0.53}Ti_{0.47})O_3$ powder obtained from identical precursor solutions. Thus, the PbO covercoat facilitated crystallization of single-phase perovskite material. As $Pb(Zr_{0.53}Ti_{0.47})O_3$ is on the MPB, more than one crystal symmetry could be present (traditionally assigned to rhombohedral or tetragonal systems).[24] Theoretically, the perovskite (200) reflection, which appears as a single broad peak in the current data, should contain three separate peaks (two from the tetragonal phase and one from the rhombohedral phase) if crystal symmetry mixing were present. However, as peak splitting or peak shoulders were not observed, pseudocubic peak

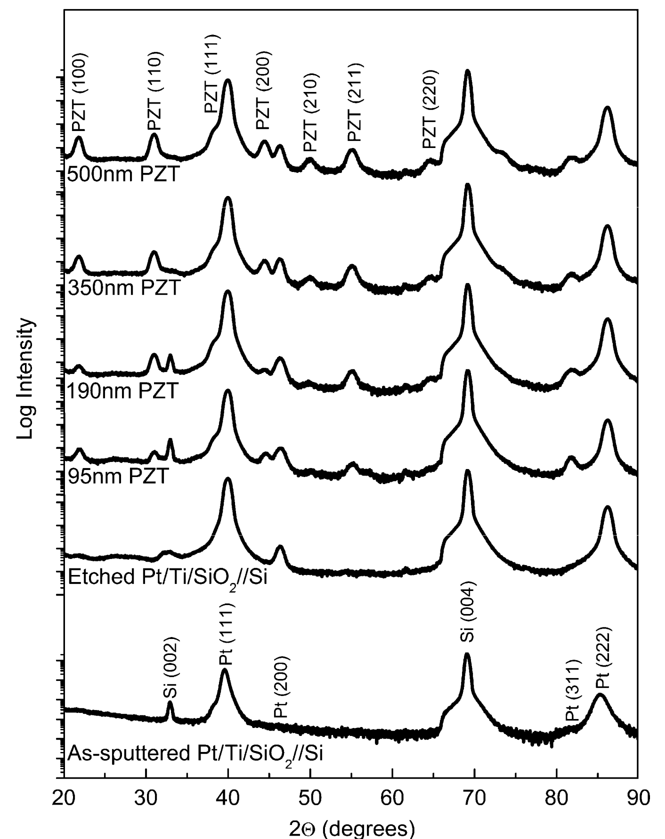

Fig. 4. X-ray diffraction data (2θ–ω) for PZT films crystallized on $Pt/Ti/SiO_2//Si$ substrates.

assignments were made. Previous research has used XRD to determine the presence and relative proportion of *a*- and *c*-type ferroelectric domains aligned in tetragonal PZT films, as the presence of (100), (001), and (111) reflections were then clearly discernable.[27] Measured dielectric data were related to the relative intensities of the peaks and the intrinsic K_i values for those directions. In the present work, for $Pb(Zr_{0.53}Ti_{0.47})O_3$, the composition for the MPB, no peak splitting or peak shoulders were detected, and domain orientation could not be confirmed for the pseudocubic material.

Furthermore, in Fig. 4, the overall perovskite peak intensity increases with increasing film thickness, while weaker substrate peaks (e.g., Si (002)) decrease in intensity. Identical scan conditions were used, and thus the observed intensity was expected to change in proportion to the thickness of the film present and the substrate available for diffraction. High-intensity Si (004) and Pt (111) peaks were noted, confirming the substrate as the expected (00*l*)-oriented Si, with a nominally (111)-textured Pt metallization layer. Additionally, a shift in the position of the Pt (111) peak was observed between the "as-sputtered" and recovered (post-PZT etched) $Pt/Ti/SiO_2//Si$ specimens. Previously, this shift from 2.27 to 2.25 Å (reduced (111) *d*-spacing) was attributed either to the formation of a Pt_3Ti phase or a change in stress state in the electrode layer during heat treatment.[46] It has been suggested that the presence of Ti near the surface of the Pt/Ti electrode layer (possibly in the form of Pt_3Ti) serves as a template for the formation of (111)-oriented PZT material. This would occur by a combination of a lowered interfacial energy between PZT and the metallic electrode layer, and a lattice mismatch of $\sim$4% between the PZT and Pt/Ti ($a = 3.94$ Å for "as-sputtered" Pt/Ti, $a = 3.90$ Å for heat-treated Pt/Ti, $a = 4.07$ Å for PZT). Previous work attempted to circumvent the reaction between Pt and Ti by direct deposition of PZT on $Pt/SiO_2//Si$ substrates. As mentioned, poor adhesion of the metallization layer to the substrate gave inferior lifetimes for $PZT/Pt/SiO_2//Si$.[23] Mechanical integrity was not found to be an issue with the current $PZT/Pt/Ti/SiO_2//Si$ specimens.

Note that regardless of film thickness, all cubic perovskite diffraction lines were observed and that only their relative intensity, not presence, changed. Powder diffraction files indicate that the (110) reflection should be the most intense, followed by the (100), (111), and (200) lines which typically are between one-tenth and one-quarter of the maximum observed intensity. This is clearly not the case for the current films. The perovskite (111) is the most intense peak in all cases even though the true intensity is partially masked by the Pt (111) peak. However, the relative intensity of the (111) peak decreases in relation to the other diffraction lines for PZT as film thickness increases. A Lotgering factor, based on a comparison between the measured diffraction patterns and that expected for a randomly oriented powder, gives the clearest indication of a trend.[47] In the present case, taking into account the (110), (111), and (200) reflections only, a (111) Lotgering factor ($f_{(111)}$) of 1.0 would indicate complete (111) orientation, while a value of 0.0 results for a purely random distribution. A negative value of a Lotgering factor indicates the experimentally observed relative intensity of that diffraction line is less than expected from the powder diffraction file. The 95 and 190 nm films had a $f_{(111)} \sim 0.74$. A value of $\sim$0.45 was calculated for the 350 and 500 nm films, indicating that the films were all nominally (111) oriented, but less so as thickness increased. Lotgering factors for the (110) orientation varied from ~ -0.59 to ~ -0.22 as the film thickness increased. Concurrently, $f_{(200)}$ changed from ~ -0.15 to ~ -0.09. Thus, an increase in the fraction of (110) and (200) orientation increased with thickness, with a larger proportion for (110).

XRD pole figures (not shown here) also verify this trend. The (111) pole figure had the highest central intensity in all films, but both (110) and (200) pole figures displayed increased central intensities as thickness increased. This phenomenon can be directly related to the processing steps involved in forming films with increasing thickness. The 95 and 190 nm thick films were deposited directly onto the (111) textured $Pt/Ti/SiO_2//Si$ substrate resulting in a strong templating effect ($f_{(111)} \sim 0.74$). In order to obtain the 350 and 500 nm films, successive depositions and thermal-processing cycles were necessary. As film thickness increased, the templating effect from the (111) fiber-textured $Pt/Ti/SiO_2//Si$ substrate decreased. Instead, self-templating from previously crystallized PZT layers occurred.

Successive deposition and heat treatment of sol–gel-derived PZT films on $Pt/Ti/SiO_2//Si$ substrates with use of a PbO cover-coat led to films of varying thickness with consistent phase content, grain size, and nominal (111) orientation. A determination of domain orientation was not feasible as peak splitting was not observed via XRD. Residual stress was tensile in all cases: 180 MPa for $t_f < 200$ nm, and 150 MPa for $t_f > 200$ nm (Fig. 1), with a calculated constrained strain of 0.3%, close to the strain to failure. The presence of such stress/strain levels and variations in film thickness may affect the properties of integrated PZT.

The dielectric properties of $PZT/Pt/Ti/SiO_2//Si$ specimens were observed to vary as a function of thickness at room temperature. Figure 5 illustrates the frequency dependence of the calculated values of dielectric constant ($\bar{K}'$) at room temperature, obtained from capacitance and geometry data. There was no significant dispersion in $\bar{K}'$, and tan δ values were typically less than 3%, and often less than 2%. $\bar{K}'$ increased with increasing thickness, from $\bar{K}' = 600$ at 95 nm to $\bar{K}' = 760$ for 190 nm, and to $\bar{K}' = 960$ at 350 nm, and remained close to this value at $\bar{K}' = 940$ at 500 nm, when measured at 50 mV AC, 100 kHz. Saturation in $\bar{K}'$ at 350 and 500 nm occurred when measured residual σ decreased to 150 MPa.

As mentioned previously, studies have shown that a 30 MPa change in applied stress results in only a 2% change in $\bar{K}'$.[10] A similar difference in stress is noted between 190 and 350 nm specimens in the present study, with a concurrent change in the room temperature $\bar{K}'$ from 760 to 960. This difference (>20%) appears to be too much to be accounted for by a difference in σ alone. A plausible explanation for the decrease in $\bar{K}'$ observed with decreasing thickness is series dilution, where series connected impedance boundaries could adversely dilute the influence of the higher $\bar{K}'_1$ major phase. Additional phases (other than perovskite) were not detected by XRD or SEM, but their presence cannot be discounted, e.g., at the Pt/Ti interface or between the PZT grains. Figure 6 analyzes dielectric data as a two-layer model. Recall that the thinnest film was one grain thick, and the calculated data in Fig. 6 fit series dilution, where the secondary contribution was modeled on the electrode interface. For thicker films, where the number of grain boundaries increases, there was no deviation from the two-layer model, i.e., there appeared to be no significant contribution from grain interfaces. This may be consistent with crystallization from a dense amorphous film, rather than from grain boundaries resulting from the sintering of particles. In any event, the data are

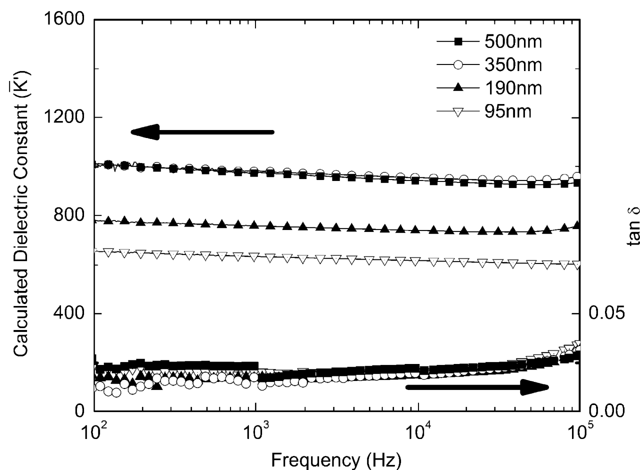

Fig. 5. Calculated room-temperature dielectric constant and tan δ of PZT films as a function of frequency and thickness.

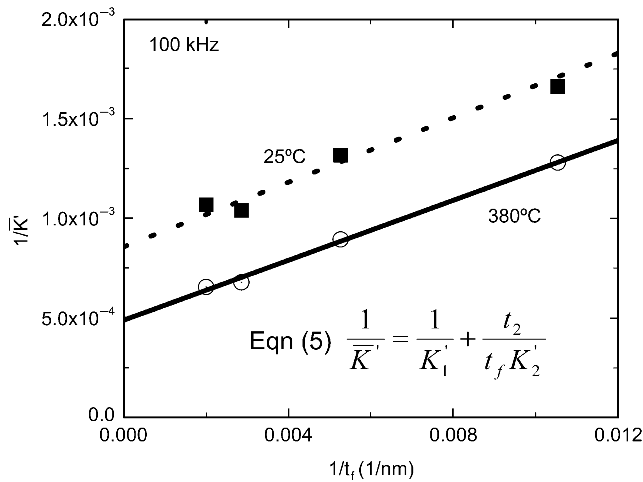

Fig. 6. Dielectric analysis of PZT films according to a series-dilution model.

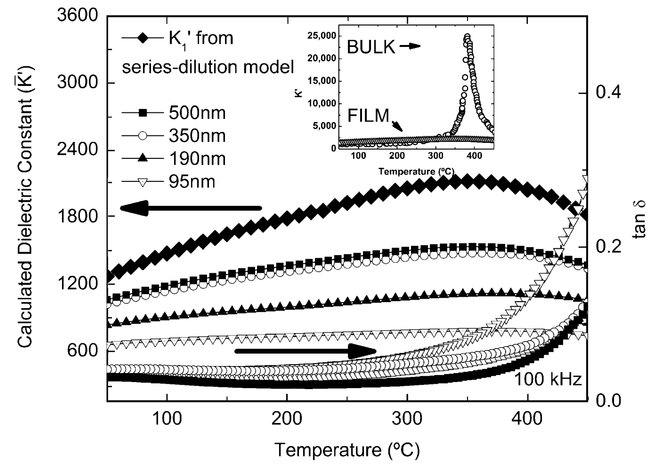

Fig. 7. Temperature dependence of dielectric response for integrated PZT films.

consistent with capacitors in series, where the secondary contribution is attributed to interfacial capacitance. Thus, the measured capacitance $\bar{C}$ is interpreted in terms of the capacitance of the major phase C_1 that is diluted by an effective impedance boundary of capacitance C_2,

$$\frac{1}{\bar{C}} = \frac{1}{C_1} + \frac{1}{C_2} \tag{3}$$

and

$$C_i = \frac{\varepsilon_0 K_i' A}{t_i} \tag{4}$$

ε_0 is the permittivity of free space, K_i' is the dielectric constant, A is the area of the electrode, and t_i is dielectric thickness. For capacitors in series,

$$\frac{1}{\bar{K}'} = \frac{1}{\bar{K}_1'} + \frac{t_2}{t_f K_2'} \tag{5}$$

where the film thickness $t_f = t_1 + t_2$, and $t_f \sim t_1$. Figure 6 gives series analysis for PZT films on Pt/Ti/SiO_2//Si. From the intercept $K_1' = 1170$ for $Pb(Zr_{0.53}Ti_{0.47})O_3$, and this constant value (now independent of thickness) is in good agreement with bulk ceramics and thicker films of similar composition.[8,24] The results verify that any differences in domain orientation, if at all present, have little effect on K_1' for the MPB composition. Additionally, the gradient is linear ($t_2/K_2' = 0.08$), indicating a constant series impedance, corresponding to K_2' values of 12 and 60 for estimates of $t_2 = 1$ and 5 nm, respectively. The exact nature of the interfacial capacitance remains unresolved, but is likely related to the electrode interface.[25] (The K_2' value would be double if two surfaces layers were in series, i.e., $2t_2$.) Recall that stress differences similar to those observed in these films (30 MPa) were reported to have only a minor effect (3%) on the room temperature K' in PZT films.[10] It is clear that a series-dilution model is consistent with the observed decrease in dielectric constant with decreasing film thickness at room temperature.

Cheng *et al.*[4] reported on the temperature dependence of $\bar{K}'$ for selected PZT compositions and temperatures. Their films had peak dielectric constants of ~3200 for a ~0.4 μm film and ~4800 for a ~3.9 μm film. The peak values occurred at different temperatures (340° vs 355°C). It was suggested that the presence of residual stress could induce a shift in Curie temperature, and a broadening of the dielectric anomaly because of phase coexistence. The effects of thickness and stress were not considered. In our work, $\bar{K}'$ and tan δ were measured as a function of temperature to gain further insight into these potential effects. As a series-dilution model appears valid for $\bar{K}'$ values at room temperature, similar results would be expected at any other temperature. Figure 6 gives additional analysis at 380°C for which a peak K_1' value of 2050 was obtained. The gradient shows there is no significant change in ratio between t_2 and K_2', i.e., a constant interfacial impedance factor persists.

Bulk ceramics of this composition have a well-defined phase transformation near 380°C. Figure 7 illustrates this is clearly not the case for films, where a broad dielectric anomaly is observed. Tan δ begins to increase above 300°C, in accordance with thermally activated conductivity. Series dilution of $\bar{K}'$ is possible at all temperatures. The K_1' phase should behave independently of the series contribution (K_2'). That is, if there is any temperature dependence of K_1', that behavior should be retrievable from the intercept of $1/\bar{K}'$ versus $1/t_f$ at each measurement temperature. This temperature dependence is expected to be similar to that observed in coarse-grain bulk ceramics of a similar composition (see inset in Fig. 7).[6] The upper trace in Fig. 7 (denoted by diamonds) shows the calculated values of K_1' for PZT films from 1170 at 25°C to 2050 at 380°C after correcting for contributions from K_2'. To the best of our knowledge, this is the first time that such a model has been applied in an attempt to recover the temperature dependence of K_1' for PZT films.

Figure 7 compares the commonly observed phase transformation around 380°C for bulk PZT ceramics plotted with the calculated K_1' data for the present specimens.[6] Randall *et al.*[6] prepared PZT ceramics with decreasing grain size and observed a decrease in $\bar{K}'$. When the simple series-dilution model is applied to their data, correcting for the contribution of K_2', a maximum K_1' of 31 000 is calculated at 380°C. This is not the case for our films in the current study. The series-dilution model cannot completely account for the observed dielectric constant behavior as a function of temperature, especially in the region of the transformation. At room temperature, the series dilution can readily explain the decrease in $\bar{K}'$ with decreasing thickness. However, a K_1' value less than one-tenth of the bulk data is obtained at the transformation temperature. A fundamental difference is shown to exist in the temperature-dependent behavior of PZT films and bulk ceramics. Heretofore, the presence of residual stress in films has not been considered for effects on the dielectric behavior as a function of temperature, and it appears to be the only remaining variable. In line with studies on the effects of pressure on perovskite single crystals,[48] it can be considered that residual tensile stress will impact the overall reduction in magnitude of K_1', and suppression of the dielectric anomaly. The interplay of stress and thickness combine to reduce the values calculated for $\bar{K}'$ at room temperature, and to broaden the dielectric anomaly as a function of temperature.

V. Conclusions

$Pb(Zr_{0.53}Ti_{0.47})O_3$ films of varying thicknesses were integrated onto Pt/Ti/SiO_2//Si substrates with constant *chemical composition* and *phase content*. The average *grain size* was approximately ~110 nm. The predominant *crystallographic orientation* was (111), attributable to a templating effect from the substrate. However, as film thickness increased, $f_{(111)}$ decreased from ~0.74 to ~0.45. A laser-reflectance method was used to measure wafer curvature before and after PZT deposition and heat treatment. Reactions that occurred on heating Pt/Ti/SiO_2//Si affected the baseline curvature, and these effects had to be accounted for in the calculation of residual stress. Tensile stresses between 180 and 150 MPa were calculated from the Stoney equation for films with thicknesses ranging between 95 and 500 nm. The residual stresses are consistent with previously published studies, and with estimates from thermal expansion mismatch between PZT and Si, and for constrained shrinkage on drying and densification. The PZT films were of high dielectric quality, with low losses and negligible frequency dispersion. Observed decreases in calculated values of dielectric constant with decreasing thickness were consistent with a series-dilution model. As such, it appeared that residual stress had only a minor effect on $\bar{K}'$ at room temperature. This is not necessarily the case for piezoelectric properties to be reported later.[49] At temperatures associated with the phase transformation, the suppression of the dielectric anomaly could not be completely accounted for by series dilution. Instead, it appears that tensile stress in the film resulted in a broadened dielectric anomaly and reduced the temperature coefficient of capacitance for integrated PZT dielectrics (compared with bulk PZT of the same composition).

Acknowledgments

Research for this publication was carried out in the Center for Microanalysis of Materials, University of Illinois at Urbana-Champaign. The authors thank V. Petrova and M. Sardela for assistance with electron microscopy and X-ray diffraction, and J. Grindley and P. Mahoney for assistance with dielectric measurements.

References

[1]A. J. Moulson and J. M. Herbert, *Electroceramics: Materials, Properties, Applications*. Chapman & Hall, London, 1990.

[2]N. Setter, "Electroceramics: Looking Ahead," *J. Eur. Ceram. Soc.*, **21**, 1279–93 (2001).

[3]S. Trolier-McKinstry and P. Muralt, "Thin Film Piezoelectrics for MEMS," *J. Electroceram.*, **12** [1–2] 7–17 (2004).

[4]J. R. Cheng, W. Y. Zhu, N. Li, and L. E. Cross, "Dielectric Properties of (100) Textured Thick $Pb(Zr_xTi_{1-x})O_3$ Films with Different Zr/Ti Atom Ratios," *J. Appl. Phys.*, **91** [9] 5997–6001 (2002).

[5]C. D. E. Lakeman and D. A. Payne, "Processing Effects in the Sol–Gel Preparation of PZT Dried Gels, Powders, and Ferroelectric Thin Layers," *J. Am. Ceram. Soc.*, **75** [11] 3091–6 (1992).

[6]C. A. Randall, N. Kim, J.-P. Kucera, W. Cao, and T. R. Shrout, "Intrinsic and Extrinsic Size Effects in Fine-Grained Morphotropic-Phase-Boundary Lead Zirconate Titanate Ceramics," *J. Am. Ceram. Soc.*, **81** [3] 677–88 (1998).

[7]X. H. Du, J. Zheng, U. Belegundu, and K. Uchino, "Crystal Orientation Dependence of Piezoelectric Properties of Lead Zirconate Titanate Near the Morphotropic Phase Boundary," *Appl. Phys. Lett.*, **72** [19] 2421–3 (1998).

[8]C. D. E. Lakeman and D. A. Payne, "Apparent Thickness Effect on Properties of Ferroelectric PZT Thin Layers," *Ferroelectrics*, **152**, 145–50 (1994).

[9]G. A. C. M. Spierings, G. J. M. Dormans, W. G. J. Moors, M. J. E. Ulenaers, and P. K. Larsen, "Stresses in Pt/Pb(Zr,Ti)O_3/Pt Thin-Film Stacks for Integrated Ferroelectric Capacitors," *J. Appl. Phys.*, **78** [3] 1926–33 (1995).

[10]T. J. Garino and H. M. Harrington, "Residual Stress in PZT Thin Films and its Effect on Ferroelectric Properties"; pp. 341–7 in *Ferroelectric Thin Films II Symposium. Materials Research Society Symposium Proceedings*, **Vol. 243**, Edited by A. I. Kingon, E. R. Myers, and B. A. Tuttle. Materials Research Society, Boston, MA, 1992.

[11]J. F. Shepard Jr., S. Trolier-McKinstry, M. A. Hendrickson, and R. Zeto, "Properties of PZT Thin Films as a Function of In-Plane Biaxial Stress"; pp. 161–5 in *ISAF '96. Proceedings of the Tenth IEEE International Symposium on the Applications of Ferroelectrics*, **Vol. 1**, Edited by B. M. Kulwicki, A. Amin, and A. Safari. IEEE, East Brunswick, NJ, 1996.

[12]L. Lian and N. R. Sottos, "Stress Effects in Sol–Gel Derived Ferroelectric Thin Films," *J. Appl. Phys.*, **95** [2] 629–34 (2004).

[13]L. L. Zhang, J. Tsaur, and R. Maeda, "Residual Stress Study of SiO_2/Pt/Pb(Zr,Ti)O_3/Pt Multilayer Structure for Micro Electro Mechanical System Applications," *Jpn. J. Appl. Phys. Part 1 — Regul. Pap. Short Notes Rev. Pap*, **42** [3] 1386–90 (2003).

[14]R. Thomas, S. Mochizuki, T. Mihara, and T. Ishida, "Preparation of Pb(Zr,Ti)O_3 Thin Films by RF-Magnetron Sputtering with Single Stoichiometric Target: Structural and Electrical Properties," *Thin Solid Films*, **413**, 65–75 (2000).

[15]M. C. Kim, J. W. Choi, S. J. Yoon, K. H. Yoon, and H. J. Kim, "Thickness Dependence of $Pb(Zr_{0.52}Ti_{0.48})O_3$ Films Prepared by Pulsed Laser Deposition," *Jpn J. Appl. Phys.*, **41** [Part 1 6A] 3817–21 (2002).

[16]S. Yokoyama, T. Ozeki, T. Oikawa, and H. Funakubo, "Preparation of Orientation-Controlled Polycrystalline Pb(Zr, Ti)O_3 Thick Films on (100) Si Substrates by Metalorganic Chemical Vapor Deposition and their Electrical Properties," *Jpn. J. Appl. Phys.*, **41** [Part 1, 11B] 6705–8 (2002).

[17]Z. Wei, K. Yamshita, and M. Okuyama, "Preparation of $Pb(Zr_{0.52}Ti_{0.48})O_3$ Thin Films at Low-Temperature of Less than 400°C by Hydrothermal Treatment Following Sol–Gel Deposition," *Jpn. J. Appl. Phys.*, **40** [Part 1, 9B] 5539–42 (2001).

[18]J.-P. Maria, K. Cheek, S. Streiffer, S.-H. Kim, G. Dunn, and A. I. Kingon, "Lead Zirconate Titanate Thin Films on Base-Metal Foils: An Approach for Embedded High-Permittivity Passive Components," *J. Am. Ceram. Soc.*, **84** [10] 2436–8 (2001).

[19]K. D. Budd, S. K. Dey, and D. A. Payne, "Sol–Gel Processing of $PbTiO_3$, $PbZrO_3$, PZT, and PLZT Thin Films," *Proc. Br. Ceram. Soc.*, **36**, 107–21 (1985).

[20]C. J. Brinker and G. W. Scherer, *Sol–Gel Science: The Physics and Chemistry of Sol–Gel Processing*. Academic Press, San Diego, 1990.

[21]J. S. Wright and L. F. Francis, "Phase Development in Si Modified Sol–Gel-Derived Lead Titanate," *J. Mater. Res.*, **8** [7] 1712–20 (1993).

[22]R. J. Ong and D. A. Payne, "Chemical Solution Deposition of PZT Thin Layers on Silicon: Densification and Stress Development," *Br. Ceram. Trans.*, **103** [2] 97–100 (2004).

[23]R. J. Ong, "Chemical-Solution Derived Pb(Zr0.53Ti0.47)O_3 Thin Layers: Densification and Stress Evolution"; M.S., University of Illinois at Urbana-Champaign, Urbana, IL, 2001.

[24]B. Jaffe, W. R. Cook, and H. Jaffe, *Piezoelectric Ceramics*. Academic Press, London, 1971.

[25]P. K. Larsen, G. J. M. Dormans, D. J. Taylor, and P. J. van Veldhoven, "Ferroelectric Properties and Fatigue of $PbZr_{0.51}Ti_{0.49}O_3$ Thin Films of Varying Thickness: Blocking Layer Model," *J. Appl. Phys.*, **76** [4] 2405–13 (1994).

[26]M. H. Frey, Z. Xu, P. Han, and D. A. Payne, "The Role of Interfaces on an Apparent Grain Size Effect on the Dielectric Properties for Ferroelectric Barium Titanate Ceramics," *Ferroelectrics*, **206–220**, 337–53 (1998).

[27]G. L. Brennecka, W. Huebner, B. A. Tuttle, and P. G. Clem, "Use of Stress to Produce Highly Oriented Tetragonal Lead Zirconate Titanate (PZT 40/60) Thin Films and Resulting Electrical Properties," *J. Am. Ceram. Soc.*, **87** [8] 1459–65 (2004).

[28]T. Kumazawa, Y. Kumagai, H. Miura, M. Kitano, and K. Kudshido, "Effect of External Stress on Polarization in Ferroelectric Thin Films," *Appl. Phys. Lett.*, **72** [5] 608–10 (1998).

[29]I. Kanno, Y. Yokoyama, H. Kotera, and K. Wasa, "Thermodynamic Study of c-Axis-Oriented Epitaxial Pb(Zr,Ti)O_3 Thin Films," *Phys. Rev. B*, **69**, 064103-1-7 (2004).

[30]W. R. Buessem, L. E. Cross, and A. K. Goswami, "Phenomenological Theory of High Permittivity in Fine-Grained Barium Titanate," *J. Am. Ceram. Soc.*, **49** [1] 33–6 (1966).

[31]W. R. Buessem, L. E. Cross, and A. K. Goswami, "Effect of Two-Dimensional Pressure on the Permittivity of Fine- and Coarse-Grained Barium Titanate," *J. Am. Ceram. Soc.*, **49** [1] 36–9 (1966).

[32]N. A. Pertsev, A. G. Zembilgotov, S. Hoffmann, R. Waser, and A. K. Tagantsev, "Ferroelectric Thin Films Grown on Tensile Substrates: Renormalization of the Curie–Weiss Law and Apparent Absence of Ferroelectricity," *J. Appl. Phys.*, **85** [3] 1698–701 (1999).

[33]N. A. Pertsev, A. G. Zembilgotov, and A. K. Tagantsev, "Effect of Mechanical Boundary Conditions on Phase Diagrams of Epitaxial Ferroelectric Thin Films," *Phys. Rev. Lett.*, **80** [9] 1988–91 (1998).

[34]A. Emelyanov, N. A. Pertsev, and A. L. Kholkin, "Effect of External Stress on Ferroelectricity in Epitaxial Thin Films," *Phys. Rev. B-Condens. Matter*, **66**, 214108 (2002).

[35]S. H. Oh and H. M. Jang, "Two-Dimensional Thermodynamic Theory of Epitaxial Pb(Zr,Ti)O_3 Thin Films," *Phys. Rev. B*, **62** [22] 757–65 (2000).

[36]S. S. Sengupta, S. M. Park, D. A. Payne, and L. H. Allen, "Origins and Evolution of Stress Development in Sol–Gel Derived Thin Layers and Multideposited Coatings of Lead Titanate," *J. Appl. Phys.*, **83** [4] 2291–6 (1998).

[37]W. D. Kingery, H. K. Bowen, and D. R. Uhlmann, *Introduction to Ceramics*. Wiley-Interscience, New York, 1976.

[38]L. J. Neergaard, "High Dielectric Constant and Low Thermal Expansion Capacitor Materials in he Modified PZT System"; M.S., University of Illinois at Urbana-Champaign, Urbana, IL, 1987.

[39]L. Lian, "Stress and Orientation Effects in Ferroelectric Thin Films"; Ph.D., University of Illinois at Urbana-Champaign, Urbana, 2001.

[40]C. D. E. Lakeman, "Thermal Processing and the Evolution of Composition, Structure and Properties for Sol–Gel Derived PZT Thin Layers"; Ph.D., University of Illinois at Urbana-Champaign, Urbana, IL, 1994.

[41]T. Tani and D. A. Payne, "Lead Oxide Coatings on Sol Gel-Derived Lead Lanthanum Zirconium Titanate Thin Layers for Enhanced Crystallization into the Perovskite Structure," *J. Am. Ceram. Soc.*, **77** [5] 1242–8 (1994).

[42]G. G. Stoney, "The Tension of Metallic Films Deposited by Electrolysis," *Proc. R. Soc. London A*, **82**, 172–5 (1909).

[43]C. A. Klein, "How Accurate are Stoney's Equation and Recent Modifications," *J. Appl. Phys.*, **8** [9] 5487–9 (2000).

[44]ASTM E112-96. "Standard Test Methods for Determining Average Grain Size"; ASTM International, 1996.

[45]J. J. Wortman and R. A. Evans, "Young's Modulus, Shear Modulus, and Poisson's Ratio in Silicon and Germanium," *J. Appl. Phys.*, **36** [1] 153–6 (1965).
[46]T. Tani, J. F. Li, D. Viehland, and D. A. Payne, "Antiferroelectric–Ferroelectric Switching and Induced Strains for Sol–Gel Derived Lead Zirconate Thin Layers," *J. Appl. Phys.*, **75** [6] 3017–23 (1994).
[47]F. K. Lotgering, "Topotactical Reactions with Ferrimagnetic Oxides Having Hexagonal Crystal Structures—I," *J. Inorg. Nucl. Chem.*, **9**, 113–23 (1959).
[48]G. A. Samara, "Pressure and Temperature Dependence of the Dielectric Properties and Phase Transitions of the Ferroelectric Perovskites: $PbTiO_3$ and $BaTiO_3$," *Ferroelectrics*, **2**, 277–89 (1971).
[49]T. A. Berfield, R. J. Ong, D. A. Payne, and N. R. Sottos, "Residual Stress Effects on Piezoelectric Response of Sol–Gel Derived Pb(Zr(0.53)Ti(0.47)O(3)) Thin Films," Submitted to *J. Appl. Phys.* (2005). □